

Paper Wrinkle in Printing Devices

David Battat, Lexmark International, United States

Abstract

Paper wrinkle is problematic because it is system-related, occurring at the end of the development cycle when hardware has already been committed. In belt fusing paper wrinkle is more involved than in roll fusing, due to the system being less robust and due to constraints by rapid warm-up requirements. The main objectives here are to elucidate the mechanics of paper wrinkling, and to generate a methodology to mitigate wrinkle formation. The analysis addresses the concept of 'creep', the small differences in velocities between belt, paper and backup roll (BUR), the mechanics of paper feed in long rolls, and their relevance to paper wrinkle in belt fusing.

Paper wrinkle arises due to non-uniformities along the roll which ultimately affect paper feed rates. Non-uniformities are inherent to the design of the fuser; however there are ways to control wrinkling tendencies, e.g. by optimizing system rigidity, profiling the BUR surface and core, and saddling the shape of the belt, to name but a few. One objective of the analysis is to understand the behavior of the system before hardware selection has been firmed up. To this end a master wrinkle curve is generated, which describes the propensity of the system to wrinkle and the directions to mitigate the effect.

Factors Affecting Wrinkling Performance

Design factors: BUR rubber thickness, total load, roll and belt rigidities, surface temperature variations affecting rubber expansion, BUR end effects, PFA/paper coefficient of friction (CoF), hard vs. soft belt, flares in belt and BUR, inlet paper guide geometry.

Material properties: Rubber hardness, Poisson's ratio, time-dependent degradations, paper type.

Environmental factors: Moisture in sheet leading to dimensional changes, ambient temperature, reduction in paper stiffness due to high moisture content.

Application-Specific factors: Paper length (A4, legal, banner), special application media (labels, pre-printed forms, narrow media), toner coverage (low, high, CoF), duplex applications (CoF changes, curl).

Wrinkle Formation

Two approaches may be used to analyze wrinkle. In the first, one tests to model, e.g. Matsumoto et al [1], and in the second, one models to test and verify. An examination of the phenomenon of paper wrinkle between belt and BUR leads to two hypotheses for the cause of wrinkling:

1. *Uneven longitudinal feed rate* of the paper through the belt/BUR; in particular, feed rate at the edges slower than in the center would lead to wrinkling.
2. *Uneven transverse feed rate* caused by a velocity component in axial direction (e.g. due to skew).

Two causes of wrinkling may be identified in connection with the first hypothesis: uneven loading along the length of the roll leading to a variation in nip width, and

extension of the edges of the paper compared with center due to uneven absorption of moisture. Both cases could lead to a feed rate which is effectively slower at the edges than in the center. In this paper, quantitative assessments of the feed rates are based on analysis of the influence of the deformation of both the rubber-covered BUR and the belt, or paper, upon the feed rate.

Initially, the mechanics of paper feed rates in 2D is examined. The concepts of free and tractive rolling are introduced: the former occurs when the nip transmits zero net traction (there is traction in the nip but the sum is zero), while the latter takes place when the nip has to transmit a finite shear force such as that due to belt retardation caused by grease viscosity. The significance of the free rolling creep and tractive rolling becomes clear when the mechanics of paper feed in 3D is examined relative to long rolls, and the consequences of "stitching" together the 2D variations. Whereas the belt and the backup roll rotate at constant but different speeds, the paper is fed in the nip at different speeds across its width. The determination of paper feed rates establishes the *feed speed distribution* that ultimately controls the wrinkling behavior.

The hypothesis for wrinkle formation is that wrinkle is caused by small differences in paper feed speed across the width of the sheet. *When ends feed faster than center, there is no wrinkle; when center moves faster than ends, wrinkle occurs.* Experimental evidence generally supports these hypotheses. A fusing system should have the inherent ability to accommodate dimensional variations imposed on the sheet. For example, the edges may become 1-mm longer than the middle of the sheet due to moisture variation. This change would be accommodated by a feed speed variation edge-to-center of $\Delta V/V=1 \text{ mm}/11''=0.4\%$.

Mechanics of Paper Feed in 2D

The details of a soft-on-hard nip are shown in Figure 1. The peripheral speeds of the un-deformed rubber and PFA-covered rolls are V_1 and V_2 respectively, and the paper feed velocity is V_p . In the nip, the local surface velocities of rolls and paper are modified by their elastic deformation. In particular, rubber speed changes the most.

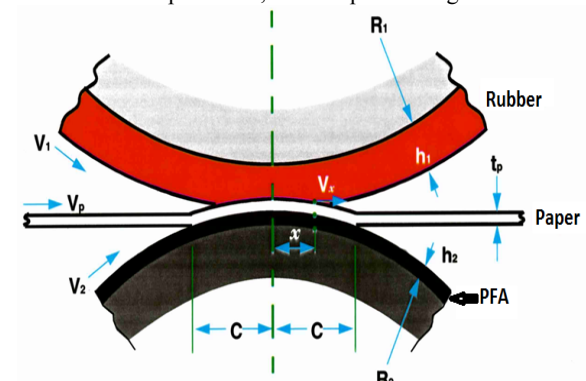


Figure 1. Velocity Details in the Nip, Upper Part, BUR, Lower Part, Belt

Creep, ξ , is defined as the maximum surface strain in the rubber, ϵ , which is also the speed difference between belt and BUR outside the nip:

$$\xi = \frac{V_{BUR} - V_{belt}}{V_{BUR}} = \frac{V_1 - V_2}{V_1} = -\epsilon \quad (1)$$

The creep equation given above arises from the condition that at the location where the BUR drives the belt, the velocities must be the same, i.e. 'speed lockup.' Two components are identified: free rolling creep due to normal loading plus zero net shear in the nip (i.e. there is shear in the nip but its sum is zero), and tractive rolling creep due to the net traction the nip has to transmit.

Free Rolling Creep

The case for the contact of a soft-covered roll loaded on a hard base was studied by Bental and Johnson [2]. Variation of free rolling creep with strip thickness and Poisson's ratio is given in Equation 2 for CoF equal 0 & ∞ .

$$(\xi)_N = \frac{V_{BUR} - V_{belt}}{V_{BUR}} = -\frac{c}{R} f(t, \mu, \nu) \quad (2)$$

$$B = \frac{1}{t} = \frac{h}{c}$$

The creep function, $f(t, \mu, \nu)$, is plotted in Figure 2. As an example, for $R=20$ mm, $h=5$ mm, nip $2c=10$ mm, and Poisson's ratio 0.5, then $B=1$, $f=0.24$ and $(\xi)_N = -0.06$, hence BUR moves slower than the belt by 6%.

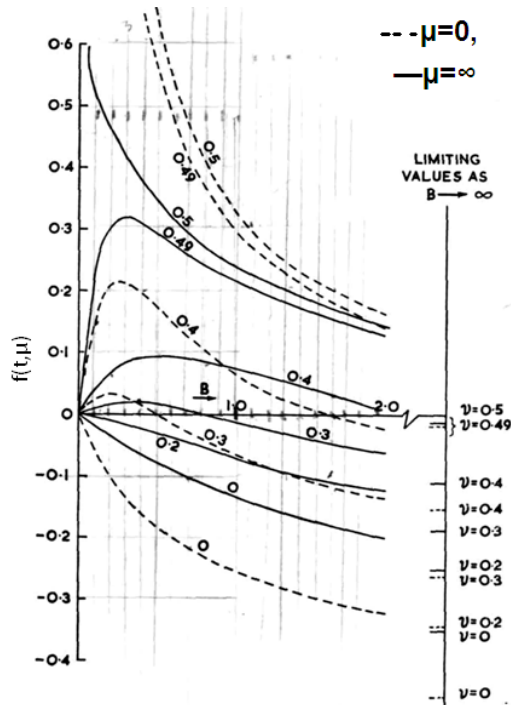


Figure 1. Free Rolling Creep variation with Strip Thickness and Poisson's Ratio (Bental & Johnson, [2])

For incompressible elastomers, $\nu = 0.5$, and for $\mu \geq 0.4$, which is typical of rubber and paper, the free rolling creep can be approximated in the region $0.5 \leq t \leq 1.5$ by a linear regression in terms of $1/t$ (Equation 3):

$$(\xi_1)_N = \frac{V_{BUR} - V_p}{V_p} = -\frac{c}{R} \left(0.4 - \frac{0.15}{t} \right) \quad (3)$$

Tractive Rolling Creep

In this case, a net tangential force is transmitted across the nip, and the effect of normal loading is absent. In such circumstances, a driving torque M_1 is applied to roll (1) and a breaking torque M_2 , to roll (2); the incoming paper carries a tension T_p , Figure 3. Equilibrium requires

$$T_p = F_1 - F_2 = (M_1 / R_1) - (M_2 / R_2) \quad (4)$$

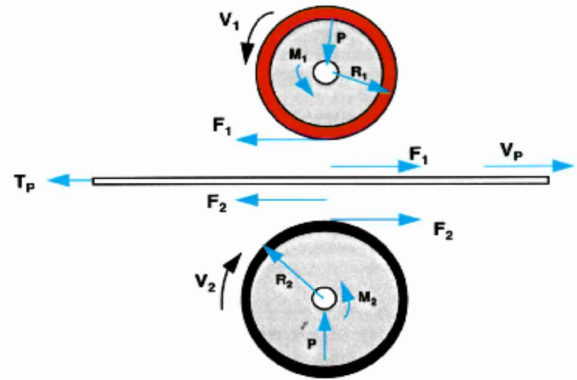


Figure 3 – Forces in the Nip

In the case of tractive rolling contact of a soft-covered roll on a homogeneous roll, the contact area divides into two zones - one at the leading edge where there is no slip and one at the trailing edge where the surfaces slip relative to each other. The extent of the slip zone spreads with increasing tangential force, and it covers the whole contact area as limiting friction force is reached. In an unpublished analysis [3], Battat, Ezra & Johnson investigated the problem by assuming two distributions of shear: one over the entire nip width to obtain slip, and one in opposite direction over a strip $2b$ where surface strain is constant. The stresses and strains are obtained from the Biharmonic equation which is solved for the prescribed loading.

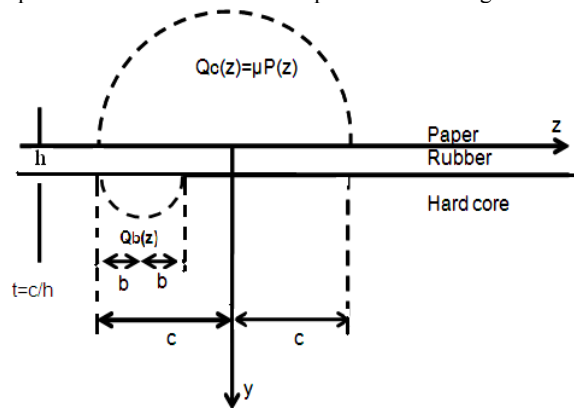


Figure 4. Tractive Force Representation in the Nip

$$Q_b(z) = -\frac{b}{c} \mu P_o \sqrt{1 - z^2/b^2}, \quad -b \leq z \leq b$$

$$Q_c(z) = \mu P_o \sqrt{1 - z^2/c^2}, \quad -c \leq z \leq c \quad (5)$$

By integrating the surface shear, a relationship is obtained between the extent of slip and the total tangential traction T :

$$T = \mu N \left(1 - \frac{b^2}{c^2}\right)$$

b/c is the fraction of the nip where lock-up takes place. When $T/\mu N=1$, the limiting friction force is reached and slip occurs throughout the contact area. When $T/\mu N=0$, then $b/c=1$, and the entire nip is a lockup region; there is no relative motion, and shear is zero.

The solution for the tractive rolling creep is given in Equation 6, with function $m(t, T/\mu N)$ shown in Figure 5.

$$(\xi_1)_T = \frac{2T(1-v^2)}{\pi E c} m(t, T/\mu N) \quad (6)$$

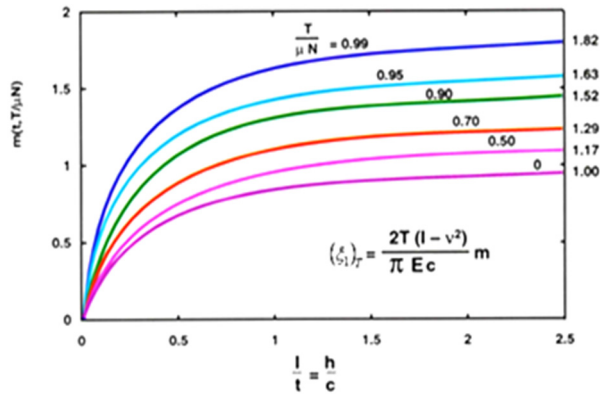


Figure 5. Tractive Rolling Creep

As an estimate of the tractive rolling creep, if $t=1$, $T/\mu N \approx 0$, then Figure 5 yields $m=0.8$. Taking rubber modulus, $E=50$ psi, and traction, $T=0.1$ lb/in, one calculates $(\xi_1)_T=0.0039$, or about 0.4%. Thus, tractive rolling creep is only 1/10 of free rolling creep, which was estimated at 6%, nevertheless it is important for paper wrinkle formation, because of the build-up as the sheet feeds through the nip.

In the linear range, $l/t=0-0.25$ of Figure 5, the tractive rolling creep may be expressed as

$$(\xi_1)_T = 1.067 \times 0.77 \frac{h}{R} t^{2.165} \frac{T}{N} \quad (7)$$

In this case, $(\xi_1)_T$ is independent of CoF at rubber/paper interface, but strongly dependent on nip.

Creep of Paper Relative to PFA in Hard Belt

A hard belt has no rubber layer. The belt is covered with a thin PFA layer, with modulus typically $\sim 100,000$ psi, which is greater than the modulus of the paper. Hence creep of paper relative to PFA will be due mostly to paper deformation, which in free rolling is investigated using a plate theory model [4]. The resulting creep function, Φ_P , and the free rolling creep are given in Equation 8 and Figure 6, which show that creep depends strongly on CoF between belt PFA and paper: creep is small for high CoF values, becoming large for small CoF values. For the hard belt case, tractive rolling creep is negligible unless $\text{CoF} \approx 0$.

$$(\xi_2)_N = \Phi_P \times \frac{P_o}{2G_P} = \frac{V_p - V_{belt}}{V_p} \quad (8)$$

P_0 =Maximum nip pressure
 G_p =Paper shear modulus = 75 MPa

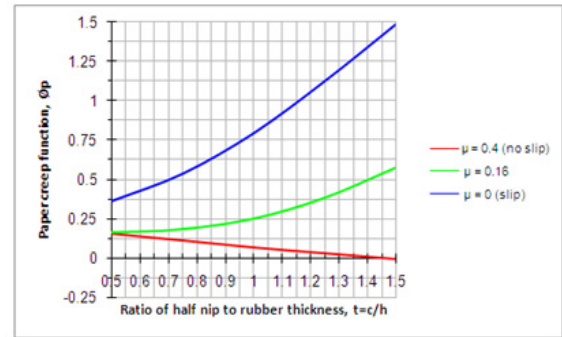


Figure 6. Paper Creep Relative to Hard Belt Depends on CoF at Belt Paper Interface

The coefficient of friction at belt/paper interface is relevant to paper slip behavior in relation to toner coverage.

- For low toner coverage ($\mu \geq 0.4$), CoF is relatively high. Paper feed speed will follow the speed of the hard belt. In this case, nip shape has little influence on paper feed rate, but belt saddling is beneficial.
- For full toner coverage ($\mu = 0$), slip occurs at belt/paper interface, preventing the paper from following the belt. In this case, paper feed rate is determined by the deformation of the BUR rubber and nip flare, but not by belt profiling.

Figure 7 shows the onset of slip for $\text{CoF}=0.02$ and nip flare= 20% . The red lines represent the ultimate local slip value $\pm \mu N(x)$, and the solid black curve gives the predicted local shear. Slip occurs both at the edges and in the middle of the roll where the predicted values are not observed, because they exceed the maximum they can achieve.

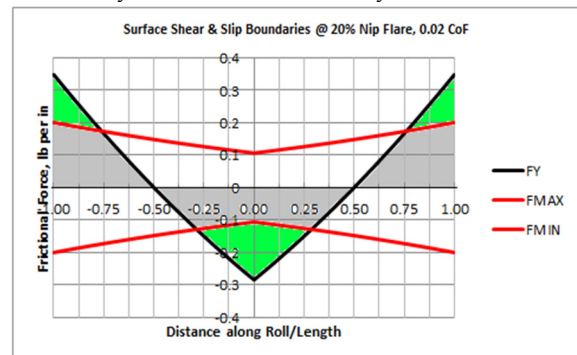


Figure 7. Effect of Nip Flare and CoF on Slip of Paper on PFA

Non-Uniform Loading of Long Rolls Variation from Ends to Center

With two long rolls, their rigid cores ensure that the creep ratio, $CR=(V_2-V_1)/V_2$, is constant along the length of the roll. The load distribution is, however, non-uniform causing the free rolling creep to vary with the local pressure, which, in turn, produces internal twisting moments so that tractive rolling would occur. This, in turn, produces tangential forces that enable the roll to rotate as one coherent unit. The tangential forces adjust themselves

to satisfy the condition that the sum of free and tractive rolling creeps is constant at all cross-sections of the rolls.

For example, if the load at the ends of the rolls is greater than that in the center and the paper tension T_p is taken to be zero, in free rolling the ends of the rubber roll would run slower than the center. Since all sections of the roll must run at the same speed, traction forces will be exerted to speed up the end sections, and opposite forces will be exerted to slow down the center sections.

Next, the combined effect of free and tractive rolling creeps on the paper feed rate, V_p , must be evaluated. To answer this question we need to know the feed rates in both free and tractive rolling since their signs will be opposed, but it seems likely that the net creep will outweigh the free rolling creep resulting in an increase in V_p where the pressure is high. Thus, increased pressure at the ends of the rolls would give rise to the sides of the paper feeding faster than the center and thereby inhibiting any tendency to wrinkle. Conversely, a higher pressure in the center would reverse these trends and lead to the middle of the sheet being fed faster than the edges, which is a wrinkling situation.

Variation from End-to-end

Higher loading at one side of the paper compared to the other side, can influence the transverse velocity of the paper. This may also be affected by profiling (tapering or flaring) the surface of the hard roll. Since paper follows closely the speed of the hard roll, a feed rate distribution may be designed by shaping the surface of the hard roll accordingly. The change in local creep obtains in terms of $\Delta R/R$, which is the fractional change in the radius. This solution may be optimized depending on the configuration, e.g. high Relative Humidity, Legal Paper, Pre-Printed form.

Skewing of the rolls is another source for non-uniformities, leading to higher loading at one side than the other, and to transverse velocities of the paper.

Variation in Properties of the Paper

Absorption of moisture into the sides of a stack of paper causes the edges of the sheet to extend with respect to the center, as evidenced by the sheets acquiring a wavy edge. This means that the paper passes through the nip in a state of effective tensile strain, ϵ_x positive, compared with its natural length. Here, the edges of the paper feed more slowly than the center, leading to wrinkling.

Determination of Paper Feed Rates in Long Rolls

The roll is conceptually divided into separate 2D rolls. Load varies along the roll due to bending, which leads to a nip distribution along the roll. Knowing the nips, free rolling creep is calculated at each 2D roll. The actual creep observed between BUR and belt would be the average free rolling creep, as shown in Figure 8. However, in order to force each section to rotate at the average creep, shear is created along the roll to slow the middle sections and to accelerate the edges, giving rise to a tractive rolling creep distribution. The shear distribution thus created satisfies the condition that the sum of free rolling creep and tractive rolling creep is constant at all sections. Knowing the creep

values, paper feed rates may be evaluated at each point, and the propensity to wrinkle determined. Figure 8 depicts the steps involved.

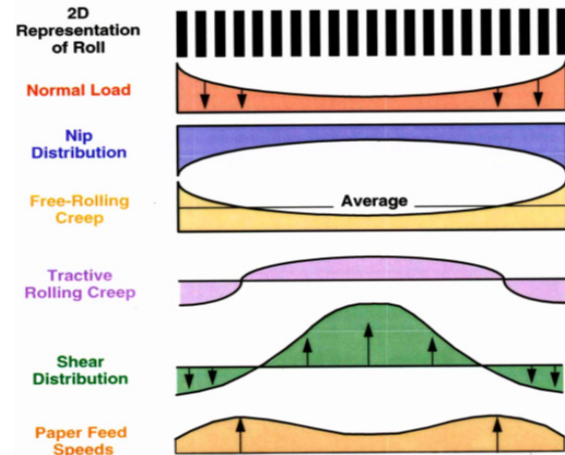


Figure 8. Long Rolls – Determination of Paper Feed Rates

Analysis yields the paper feed speed along the roll, which is given in terms of the local free rolling creep and tractive rolling creep components, as shown in Equation 9:

$$\frac{V_p(x)}{V_1} = 1 - CR_1(N;x) - CR_1(T;x) \quad (9)$$

Likewise, the shear created at a point along the axis is

$$F_1(x) = -F_2(x) = \frac{\pi}{2} \frac{c(x)}{(1-\nu^2)} \left(\frac{CR - CR_{12}(N;x)}{\left(\frac{m(t_1)}{E_1} + \frac{m(t_2)}{E_2} \right)} \right) \quad (10)$$

In Equation 10, $c(x)$ is the local half nip, CR , the net creep between belt and BUR, and $CR_{12}(N;x)$ is the difference between the free rolling creeps at both sides of the paper at a given point along the axis. Computed paper feed rates are shown in Figure 9. Plots take into account bending of the frame of the belt and BUR core, for various values of the rubber modulus. The figure includes a range in speed variation from 0.2% to 0.4% where dimensional changes in paper are accommodated. The red and blue curves fall short of having adequate wrinkle control, whereas the yellow and green curves provide satisfactory control. For robust performance, the velocity profile should monotonically increase from center to edge, implying a positive 2nd derivative of the velocity curve.

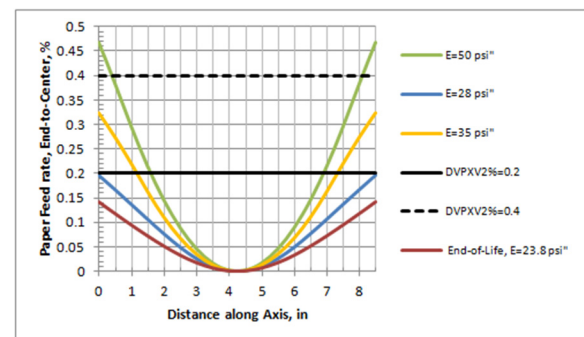


Figure 9. Paper Feed Rates for Different Operating Conditions

Paper Feed Rate Algorithm

A computational algorithm evaluated paper feed rates across the sheet for a given core and surface profile of the BUR, and a specific system rigidity. The flexure model used the analysis of beams loaded on flexible foundations [5] to determine the load, indentation and nip variations along the roll. The output of the model gives the ratio of speed difference in paper feed speed between end and center of the sheet, to the process speed, as expressed by $\Delta V_p/V$. Figures 10-12 show variations along axis in load, nip, and individual displacements, respectively.

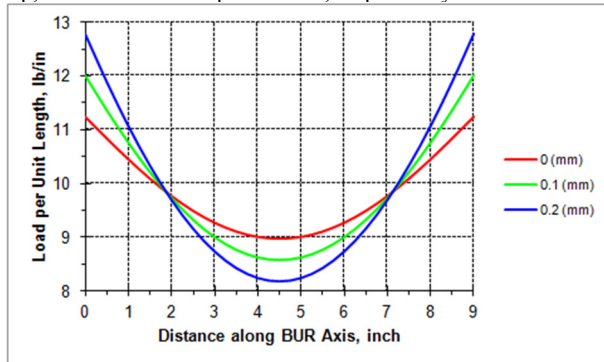


Figure 10 Load Variation along axis

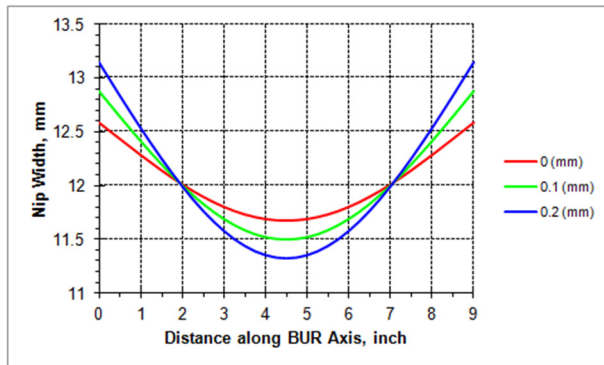


Figure 11. Nip variations along axis

The deflections of the belt frame (solid lines) are much larger than the bending of the core of the BUR (broken lines). The difference between deflection at the end and deflection at the center represents the bending of the belt frame. In this case, the difference is 0.194 mm.

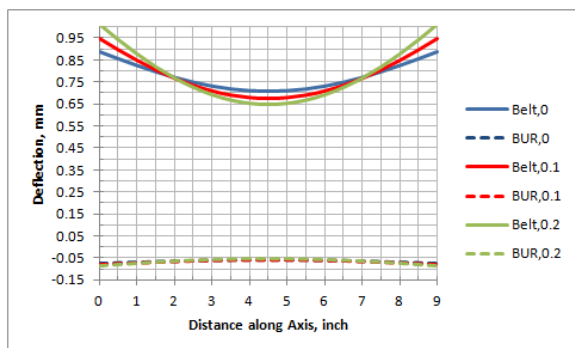


Figure 12. Individual Deflections of Belt (top) and BUR (bottom)

The metric $\Delta V_p/V$ and shear distributions are shown in Figures 13 and 14, respectively.

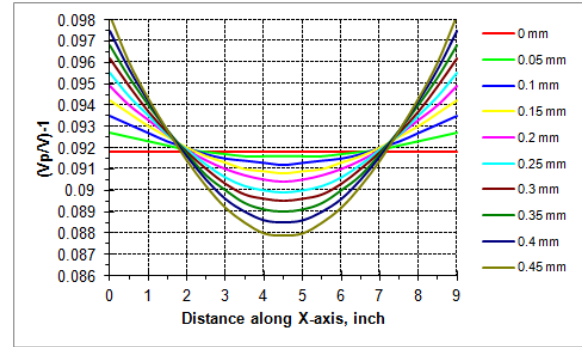


Figure 13. Paper Speed Relative to BUR Speed (e.g., 0.096 signifies paper moves at 9.6% faster than the BUR)

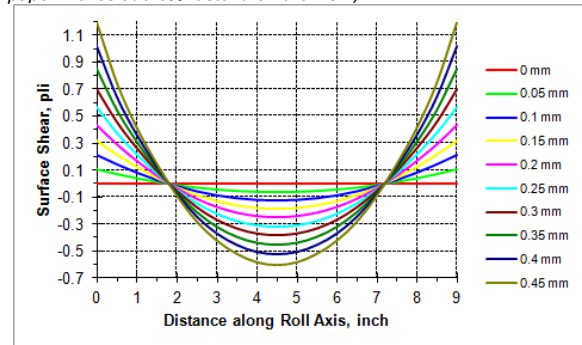


Fig 14. Axial Surface Shear Variations for Different BUR Saddles

Master Wrinkle Plot

A master wrinkle plot is introduced which shows the effect of BUR surface and core profiling on paper feed rate metric $\Delta V_p/V$. In this plot, the range 0.2%-0.4% is chosen as an optimum domain for anti-wrinkling behavior. Using the principle of superposition, other factors are accounted for in the master plot and their effect on paper feed rate is determined. Thus, effects of bending, thermal expansion, surface profiling, and end effects, can be represented dimensionally on the abscissa. By moving up vertically, one reads the required core profile needed to achieve the desired wrinkle control characteristic, within the range of 0.2%-0.4%.

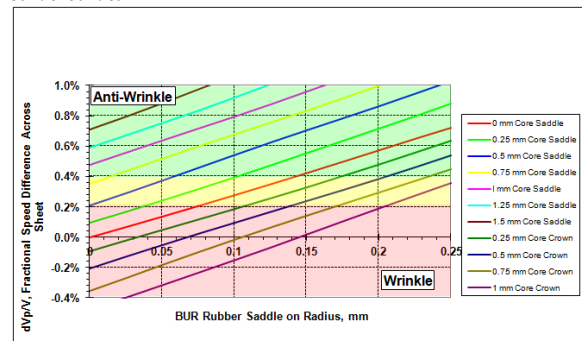


Figure 15. Feed Rates vs. BUR Surface Saddle and Core Profile

Approaches to Wrinkle Control Belt Profiling

Profiling the hard roll affects the feed speed across the width of the sheet. Belt shape flaring in belt fusing acts much the same way as a profiled hard roll. A saddle on the surface of a hard roll causes the paper to be fed at the edges

faster than in the middle. Likewise, for continuous operation of a saddled belt, the belt must rotate at a constant angular velocity, causing the edges to move at a higher speed than the center. In turn this induces higher paper speeds at edges than in the middle, Figure 16. There is also a correction due to paper deformation.

$$\frac{\Delta V_p}{V_1} = \frac{\Delta R}{R} - (\xi_2)_N \quad (10)$$

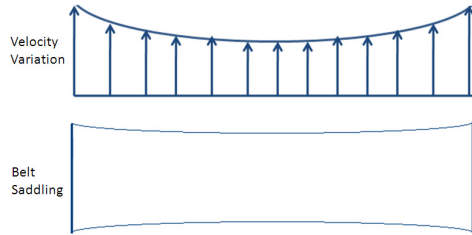


Figure 16. Profiled Belt Induces Speed Variations

Nip Flare

One way to affect paper feed rate and the metric $\Delta V_p/V$ is nip flare. For given loading conditions the softer is the roll, the larger is the nip but the lower is the nip flare, and conversely the harder is the roll the smaller is the nip but the larger is the nip flare.

Effect of Poisson's Ratio

The effect of Poisson's ratio on wrinkle is illustrated in Figure 17. The curve indicates that a system with low Poisson's ratio, e.g. foam, is 'forgiving' to changes. As ν goes down, paper feeds more uniformly, and it is easier for the system to absorb non-uniformities.

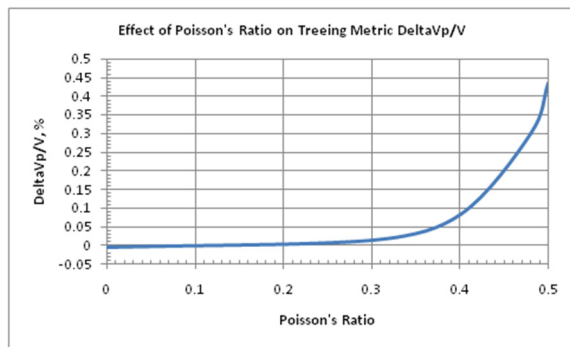


Figure 17. Effect of Poisson's Ratio on Wrinkle Metric $\Delta V_p/V$

Concluding Remarks

In principle, a "perfect system" devoid of non-uniformities, does not wrinkle. There are many sources for non-uniformities in the system; the hypothesis of this analysis is that wrinkling is caused by uneven feed rate of the paper along the contact length between belt and BUR. Analyses have been generated to estimate the influence of system non-uniformities on paper feed rate, and the effect of correction by nip changes and belt saddling, the two main countermeasure means.

Two distinct belt/BUR configurations are addressed BUR with soft belt, and BUR with hard belt. In the soft-on-soft system paper feed rates are determined by calculating the deformation of the rubber on both sides of the paper from the knowledge of the load distribution along the roll

due to bending, and profiling. In such a system both belt details and nip variation affect the paper feed rate.

In a hard belt system, the creep between paper and PFA is due to paper deformation. Some interesting observations emerge relative to toner coverage. For a high CoF at paper/PFA interface, $\mu \geq 0.4$, corresponding to low coverage, no slip occurs and the feed rate is controlled by the belt. Hence, profiling the belt is useful in this case. For a low CoF, $\mu \approx 0$ corresponding to high toner coverage, slip takes place between PFA and paper. In such a case, paper feed rates are controlled by nip variation i.e. by the BUR.

A master wrinkling plot is developed based on requiring the edges of the sheet to move uniformly faster than the center by 0.4% and taking into account various design factors such as bending, belt flaring, and BUR core and surface profiling.

References

- [1] S. Matsumoto & Y. Harada, 'Modeling of the Paper-Wrinkle Generation Process', NIP27
- [2] R.H. Bentall & K.L. Johnson, 'An Elastic Strip in Plane Rolling Contact', Int. J. Sci. **10**, 637 (1968)
- [3] D. Battat, D. Ezra & KL Johnson. Tractive Rolling Creep, Unpublished Report
- [4] Timoshenko and Young, 'Theory of Plates and Shells'
- [5] Hetenyi, 'Beams on Elastic Foundations' Ann Arbor, 1964

Author's Biography

David Battat received his DPhil in Engineering Science from Oxford University, England. He was Principal Scientist with Xerox Corporation in Webster, NY. He has worked at Lexmark International in Lexington, KY since 2007.

Notation

B	$1/t = h/c$, ratio of strip thickness to half nip
2b	No-slip width
2c	Nip Width
E	Young's modulus of rubber
E'_r	$E/(1-\nu^2)$ for rubber ≈ 5 MPa
E'_p	$E_p/(1-\nu^2)$ for paper ≈ 225 MPa
F	Tangential force
G_p	Shear modulus of paper ≈ 75 MPa
h	Rubber thickness of BUR
L	Roll length
M	Torque
N	Normal load
P	Average pressure in the nip
P_o	Peak pressure in the nip = $(4/\pi) P$
R	Radius of BUR
t	c/h , half nip to thickness ratio
t_p	Paper thickness
T	Traction or shear transmitted by nip
V_1	Peripheral speed of rubber covered roll, BUR
V_2	Peripheral speed of PFA covered roll, belt
V_p	Feed speed of paper
μ_1	Coefficient of friction at BUR/paper interface
μ_2	Coefficient of friction at belt PFA/paper interface
ν	Poisson's ratio
ξ	Net creep between BUR and belt
ξ_1	$(V_1 - V_p)/V_p$, creep at BUR/paper interface
ξ_2	$(V_p - V_2)/V_p$, creep rate at Belt/paper interface